Original Research

The effect of acoustic radiation force on osteoblasts in cell/hydrogel constructs for bone repair

James Veronick[1], Fayekah Assanah[1], Lakshmi S Nair[1,2,3,4], Varun Vyas[2], Bryan Huey[2] and Yusuf Khan[1,2,3,4]

[1]Department of Biomedical Engineering, University of Connecticut, Storrs, CT 06269-3247, USA; [2]Department of Materials Science and Engineering, University of Connecticut, Storrs, CT 06269-3136, USA; [3]Department of Orthopaedic Surgery, University of Connecticut Health Center, Farmington, CT 06030, USA; [4]Institute for Regenerative Engineering, University of Connecticut Health Center, Farmington, CT 06030, USA

Corresponding author: Yusuf Khan. Email: ykhan@uchc.edu

Abstract

Ultrasound, or the application of acoustic energy, is a minimally invasive technique that has been used in diagnostic, surgical, imaging, and therapeutic applications. Low-intensity pulsed ultrasound (LIPUS) has been used to accelerate bone fracture repair and to heal non-union defects. While shown to be effective the precise mechanism behind its utility is still poorly understood. In this study, we considered the possibility that LIPUS may be providing a physical stimulus to cells within bony defects. We have also evaluated ultrasound as a means of producing a transdermal physical force that could stimulate osteoblasts that had been encapsulated within collagen hydrogels and delivered to bony defects. Here we show that ultrasound does indeed produce a measurable physical force and when applied to hydrogels causes their deformation, more so as ultrasound intensity was increased or hydrogel stiffness decreased. MC3T3 mouse osteoblast cells were then encapsulated within hydrogels to measure the response to this force. Statistically significant elevated gene expression for alkaline phosphatase and osteocalcin, both well-established markers of osteoblast differentiation, was noted in encapsulated osteoblasts ($p < 0.05$), suggesting that the physical force provided by ultrasound may induce bone formation in part through physically stimulating cells. We have also shown that this osteoblastic response is dependent in part on the stiffness of the encapsulating hydrogel, as stiffer hydrogels resulted in reducing or reversing this response. Taken together this approach, encapsulating cells for implantation into a bony defect that can potentially be transdermally loaded using ultrasound presents a novel regenerative engineering approach to enhanced fracture repair.

Keywords: Bone, ultrasound, hydrogel, osteoblast, cell therapy, regenerative engineering

***Experimental Biology and Medicine* 2016; 241: 1149–1156. DOI: 10.1177/1535370216649061**

Introduction

Hydrogels continue to gain favor in tissue engineering and regenerative medicine as (1) tissue mimics to allow the study of cells in three-dimensional environments,[1] (2) growth factor delivery vehicles,[2] (3) synthetic extracellular matrices (ECMs) for study and implantation,[1,3,4] and (4) cell delivery and retention vehicles for cell therapy-based tissue repair.[2]

Clinically cell therapy has been used successfully for bone repair as part of autograft transplantation in which cell-enriched bone tissue harvested from the iliac crest of the patient is reimplanted at a defect site[5] and has been investigated for soft tissues as well.[6] Typically, however, these and other purely cellular approaches to tissue repair lack a way to deliver and retain cells at the defect site after implantation, lessening their beneficial attributes. Combining cell delivery with a hydrogel carrier gives the added benefit of cell persistence at the defect site[7] and custom fit to eccentrically shaped defects. Using an injectable hydrogel adds the potential for minimally invasive implantation.[8] The mechanical mismatch between hydrogels and intact bone, however, limits the utility of this approach to non-load bearing defects such as fractures and fracture non-unions. Even in these instances the fracture site requires immobilization to facilitate healing. Given that osteoblasts and their precursors respond favorably to mechanical loading overlooking this immobilization may be a missed opportunity to enhance fracture repair. With these points in mind we have been developing a strategy to mechanically load encapsulated cells within a hydrogel *after* implantation using ultrasound-generated acoustic radiation force that, if applied transdermally, would not disturb the stability of the healing fracture.

Ultrasound-generated acoustic radiation force can be delivered through a transducer at high intensities (1000 W/cm^2) and has been used to both visualize biological tissues through mechanical displacement or deformation and to assess tissue mechanical properties based on a relationship between applied acoustic force and subsequent tissue deformation, a technique referred to as elastography.[9] These acoustic waves are typically delivered in short, highly focused bursts as any longer duration would increase local temperatures to damaging levels. This risk of thermal damage therefore limits high-intensity pulses to largely non-therapeutic roles.

Low-intensity pulsed ultrasound (LIPUS), on the other hand, has been found to be clinically effective for accelerated bone fracture repair and the treatment of non-unions,[10] and while many theories have been suggested the actual mechanism behind its utility remains unknown. The existence of a measurable acoustic radiation force at high intensities suggests the possibility that at very low intensities a low level mechanical force is being applied to the fracture site. In fact one method of calibrating therapeutic ultrasound devices measures the force generated by lower intensity ultrasound, but this force has yet to be fully evaluated as a tool for loading healing bone defects. Given this, the goal of this work was to assess the mechanical nature of LIPUS at and around the intensities currently used to clinically treat fractures and bony non-unions. Here we describe (1) the design of a fully adjustable ultrasound system with user-defined ultrasound frequency, duration, and intensity; (2) the characterization of the generated intensity/pressure; and (3) the manifestation of these forces on hydrogels and cell/hydrogel constructs in culture.

Materials and methods

Collagen hydrogel preparation

Type I rat tail collagen (BD Biosciences, Franklin Lakes NJ) in acetic acid was used for collagen hydrogel preparation according to the manufacturer's protocol. Briefly, type I collagen solution was neutralized by 1 M NaOH on ice to yield the desired final hydrogel concentration. Next, 3 mL of the neutralized collagen solution was injected in each well of a six-well plate and placed in 37°C for 20 min to allow collagen solution to gel, after which the collagen hydrogels were evaluated for either physical displacement (see "Hydrogel deformation imaging" section) or used for cell culture (see "Cell culture/proliferation" section). All hydrogel preparation procedures were carried out under sterile conditions.

Ultrasound setup

LIPUS was applied to hydrogels in six-well tissue culture plates using a 1.2 MHz unfocused immersion transducer (Olympus NDT, Inc., Waltham MA), a waveform generator (Agilent Technologies, Santa Clara CA), and an ENI RF amplifier (Bell Electronics, Renton WA) and calibrated with a 200 μm diameter needle hydrophone (Onda Corp., Sunnyvale, CA). A 1 MHz carrier frequency; 1 kHz pulse repetition frequency; and either 20, 50, or 100% duty cycle were tested for output by performing an amplitude sweep on the waveform generator in order to construct intensity and pressure calibration plots which would indicate the proper input amplitude to reproduce the spatial intensity that is clinically used for fracture repair, 30 mW/cm^2.[10] To accomplish this, the transducer and hydrophone were placed underwater uniaxially 3 mm apart. The hydrophone was connected to an oscilloscope to measure output voltage, which was used to calculate pressure (kPa) for each corresponding input amplitude based on the hydrophone's calibration factor (provided by the manufacturer). The pressure was then converted to a spatial intensity (power per unit area), the measure of ultrasound commonly referred to in orthopedic clinical practice.

Hydrogel deformation imaging

Type I rat tail collagen (BD Biosciences, Franklin Lakes NJ) was formulated into four different concentrations (0.5, 0.75, 1, and 2 mg/mL) that resulted in hydrogels of four different mechanical stiffnesses. Fluorescent 1 μm beads (Fisher Scientific, Pittsburgh, PA) were encapsulated within the hydrogels and imaged with a water-cooled epifluorescent microscope (Hamamatsu Corp., Bridgewater, NJ) to track the movement of the beads under ultrasound-generated acoustic radiation force. Volocity™ acquisition and quantification software (Improvision, Inc., Coventry, UK) was used to capture the movement of fluorescent beads in each of the hydrogels during three distinct phases of testing: (1) 30 s prior to ultrasound application to establish a baseline, (2) 30 s during which the hydrogels were subjected to ultrasound treatment, and (3) 30 s after ultrasound application ended to visualize scaffold relaxation. Each concentration of hydrogel was subjected to a 20% (which corresponds to clinical treatment for bone defects), 50, and 100% duty cycle. Within each hydrogel 10 beads were tracked and their displacement in the x, y, and z planes was summed and recorded. The mean total displacement (±SD) was plotted for each concentration and duty cycle.

Cell culture/proliferation

MC3T3 mouse preosteoblast cells were obtained from ATCC (Manassas, VA) and used for proliferation and osteoblastic phenotype studies. Cells were initially cultured on tissue culture polystyrene at a seeding density of 5×10^4 cells/well in a six-well plate in α-MEM media supplemented with 10% fetal bovine serum (FBS) and 1% penicillin/streptomycin (P/S). Cells were maintained in 37°C and 5% CO_2 and medium was changed every two days.

To evaluate whether LIPUS impacted cell proliferation in hydrogels, 2.5×10^5 MC3T3 cells were encapsulated in 3 mL of 1 mg/mL (0.1%) collagen type I hydrogel concentration in six-well plates in alpha-MEM media supplemented with 10% FBS and 1% P/S. Cells encapsulated in collagen were maintained in 37°C and 5% CO_2 and medium was changed every two days. Cell cultures were treated each day with the clinical intensity of LIPUS (30 mW/cm^2) for 20 min/day (experimental group) and no LIPUS (control group) over one, three, and seven-day time points. At each time point, cells were isolated by digesting the collagen hydrogel with enzyme collagenase (Thermo Fisher Scientific,

Waltham, MA) and centrifuged to form a cell pellet. The cell pellet was re-suspended in 400 μL of PBS and 2% FBS. Propidium iodide (1 μL/400 μL) was added to each sample (n = 4 for each group) to fluorescently tag the dead cells and the total number of viable cell count was measured by magnetic-activated cell sorting (Miltenyl Biotec, Germany). One-way analysis of variance (ANOVA) statistical analysis was used to determine statistical significance between each group ($p < 0.05$).

Live dead assay

Cell/hydrogel constructs were made by encapsulating 1.0×10^5 MC3T3-E1 cells in 0.1% rat-tail Collagen Type I (BD Biosciences, #354249) as indicated above. After 24 h, the LIVE/DEAD Viability/Cytotoxicity Kit (Invitrogen, #L3224) solutions were added to the collagen scaffolds according to protocol and immediately imaged on the Zeiss LSM ConfoCor2 confocal microscope with a 10 x objective. Live cells appeared green and dead cells appeared red to indicate cell viability within the hydrogels.

Real time RT-PCR analysis

Real-time quantitative RT-PCR was performed for osteogenic markers alkaline phosphatase (AP) and osteocalcin (OC) via TaqMan gene expression assays (Thermo Fisher Scientific, Waltham, MA). After MC3T3 cells encapsulated in 1, 2, and 3 mg/mL collagen hydrogel concentration were exposed to LIPUS (30 mW/cm^2; 20% duty cycle; 1 MHz carrier frequency; 1 kHz pulse repetition frequency) cells were isolated by digesting the collagen with enzyme collagenase (Thermo Fisher Scientific, Waltham, MA) and total RNA was extracted with RNeasy Mini (Qiagen, Valencia, CA). cDNA was then synthesized using Clontech EcoDry Premix (Double Primed) reverse transcription kit (Clontech, Mountain View, CA). Amplification curves for the experimental and the control genes were recorded over the iQ5 RT-PCR machine (BioRad, Valencia, CA) and the relative gene levels between samples were quantified. Data were calculated via the delta–delta Ct method and normalized to housekeeping gene Glyceraldehyde-3-Phosphate Dehydrogenase (GAPDH) and relative to the day 1 control sample. One-way ANOVA statistical analysis was used to determine statistical significance ($p < 0.05$).

Results

Ultrasound characterization

To generate an ultrasound impulse the transducer requires an input amplitude, which manifests itself as either a spatial intensity (mW/cm^2) or a pressure (Pa). Whether the resultant impulse is expressed as a spatial intensity or pressure depends on the application at hand, but converting from one to the other is straightforward. Data were collected to generate Figure 1(a) and (b) so the desired spatial intensity or pressure could be generated and applied to cells and cell/hydrogel constructs by inputting the appropriate amplitude and duty cycle. Figure 1(a) shows the empirically derived relationship between input amplitude and spatial intensity for our system, while Figure 1(b) shows the empirically derived relationship between input amplitude and pressure, and Figure 1(c) shows the mathematically derived relationship between spatial intensity and pressure. Results indicate a positive correlation between input amplitude and both pressure and spatial intensity. That is, as input amplitude increased, transducer output (as shown by increased pressure values) increased, and increased amplitude also resulted in an increased spatial intensity.

Hydrogel deformation

Fluorescent beads encapsulated in collagen hydrogels showed clear evidence of displacement at both the onset and cessation of ultrasound, suggesting that hydrogel deformation and subsequent recovery occurred when exposed to ultrasound treatment. Figure 2 shows the mean displacement of tracked beads within hydrogels when ultrasound was turned on (at 30 s) and off (at 60 s), suggesting that when ultrasound was turned on the hydrogels underwent deformation and then were held in that position (suggested by little to no bead displacement between 30 and 60 s) until the ultrasound was turned off and the beads then moved again as the hydrogel partially recovered its original shape. Partial versus full recovery is suggested because the magnitude of the bead displacement at 60 s is less than that at 30 s. Given that these hydrogels are viscoelastic in nature the difference in displacement is to be expected.

Of the four hydrogel concentrations tested the lowest viscosity hydrogel (0.5 mg/mL collagen) experienced the highest amount of deformation for all three duty cycles (20, 50, and 100%), and for that hydrogel the 100% duty cycle showed the greatest displacement, followed by 50 and 20%. As hydrogel concentration increased from 0.5 to 2 mg/mL there was a progressive decrease in the amount of hydrogel displacement for each of the duty cycles, but the relationship between duty cycle and individual hydrogel deformation was consistent across all concentrations. The lack of hydrogel deformation with the 2 mg/mL concentration defined the upper level of stiffness that would permit deformation only for the levels of intensity evaluated in this study since applying a higher intensity to that hydrogel did show some evidence of displacement (data not shown).

Proliferation and live/dead study

The impact of LIPUS on proliferation was evaluated using gel-encapsulated MC3T3 cells over a period of seven days (Figure 3). At days 1, 3, and 7 there was no statistical difference between LIPUS and control groups indicating that the application of LIPUS neither inhibited nor stimulated proliferation within the hydrogel. Cells encapsulated within hydrogels also showed no evidence of cell death as indicated by the live/dead assay (Figure 4).

qRT-PCR

Figure 5 shows the cellular response of encapsulated MC3T3 cells encapsulated in three different hydrogel concentrations (1, 2, and 3 mg/ml) to ultrasound with a 20% duty cycle applied daily over one, three, and seven days.

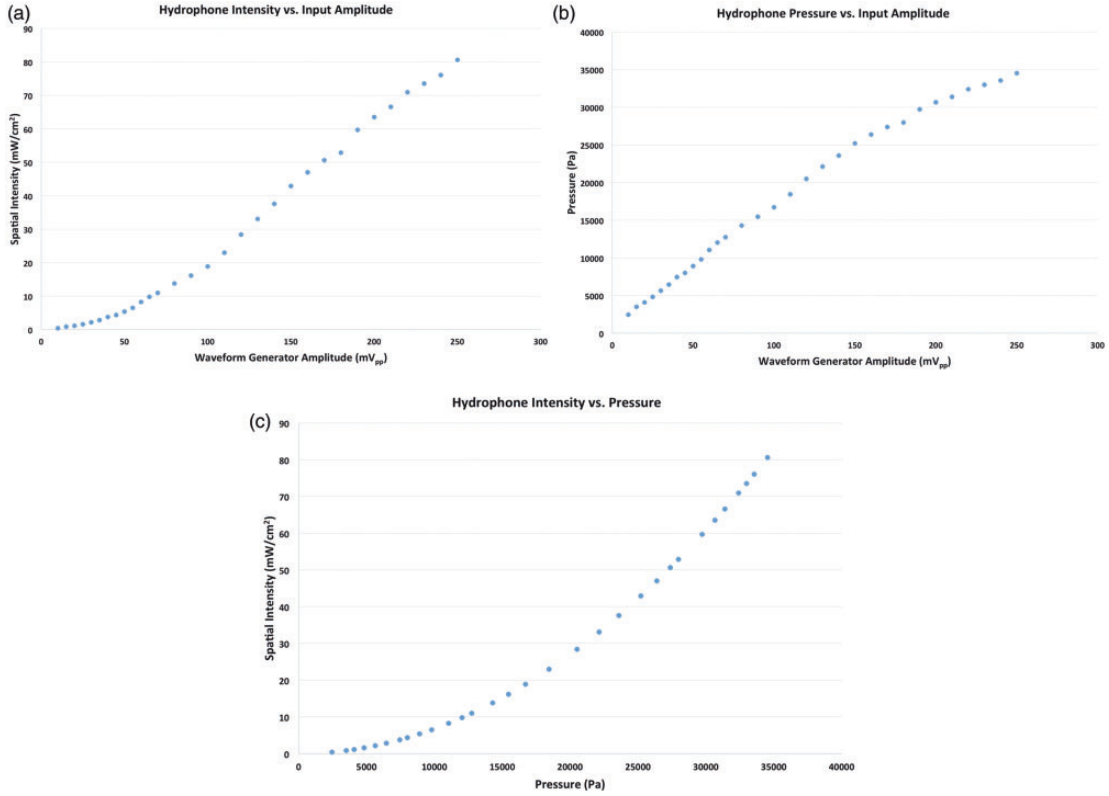

Figure 1 The relationship between input voltage to the transducer via the waveform generator and resulting spatial intensity (a) or pressure (b) output has been empirically determined by converting the measured voltage by a high-resolution hydrophone. The relationship between pressure and spatial intensity is also shown (c). (A color version of this figure is available in the online journal.)

Results indicate that after seven days cells in the softest hydrogels respond to ultrasound by expressing a statistically significant upregulation of both alkaline AP (Figure 5(a)) and OC (Figure 5(d)) gene expression, each a well-documented marker of osteoblastic differentiation, over cells in similar hydrogels not exposed to ultrasound (control). As the concentration of the hydrogel increased and deformation decreased the enhanced expression of AP mRNA from cells within the hydrogel receiving ultrasound was muted to the point where there was no difference between the two treatment groups statistically (Figure 5(b)) or numerically (Figure 5(c)), and the expression of OC mRNA was completely muted (Figure 5(f)) while encapsulated cells with no ultrasound showed an increase in OC expression.

Discussion

Every year, roughly 2.2 million bone graft procedures are performed worldwide at the considerable cost of approximately $2.5 billion per year.[11] Autografts are used for enhanced bone healing, spinal fusion, bone defects, and fracture repair and are the current gold standard for bone graft procedures.[12] However, the autograft requires a second surgery at the tissue harvest site that increases postoperative pain and the likelihood of surgical complications (donor-site morbidity). Allografts, the first alternative to autografts, account for about 43% of all bone grafts but there is a minimal but real risk of disease transmission from donor to recipient,[13,14] and high failure rates when evaluated at the 10-year mark.[15] Given the large demand and shortcomings of autografts and allografts, we and other researchers have been investigating novel strategies to find an alternative.[16–24] Regenerative engineering has great potential as a viable alternative to autografting but it is not widely available for clinical use due to both regulatory hurdles and modest healing success. Improving bone tissue engineering outcomes may accelerate acceptance and availability as a clinical tool for bone defect repair. One strategy involves looking to current, clinically accepted treatments like LIPUS and blending them with novel biomaterials-based strategies, like cell therapy combined with physically deformable hydrogel-based scaffolds, capable of delivering and localizing viable cell populations to enhance bone defect healing.[2] We have been looking at such hydrogels and have been exploring ways of mechanically loading the encapsulated cells remotely after implantation to enhance healing. One viable tool for this is ultrasound-generated acoustic radiation force.

Ultrasound, or the application of acoustic energy, is a minimally invasive technique that has been used in diagnostic, surgical, imaging, and therapeutic applications. Acoustic energy is produced from a piezoelectric crystal within a transducer that emits high-frequency acoustic pressure waves (1–12 MHz) capable of passing through

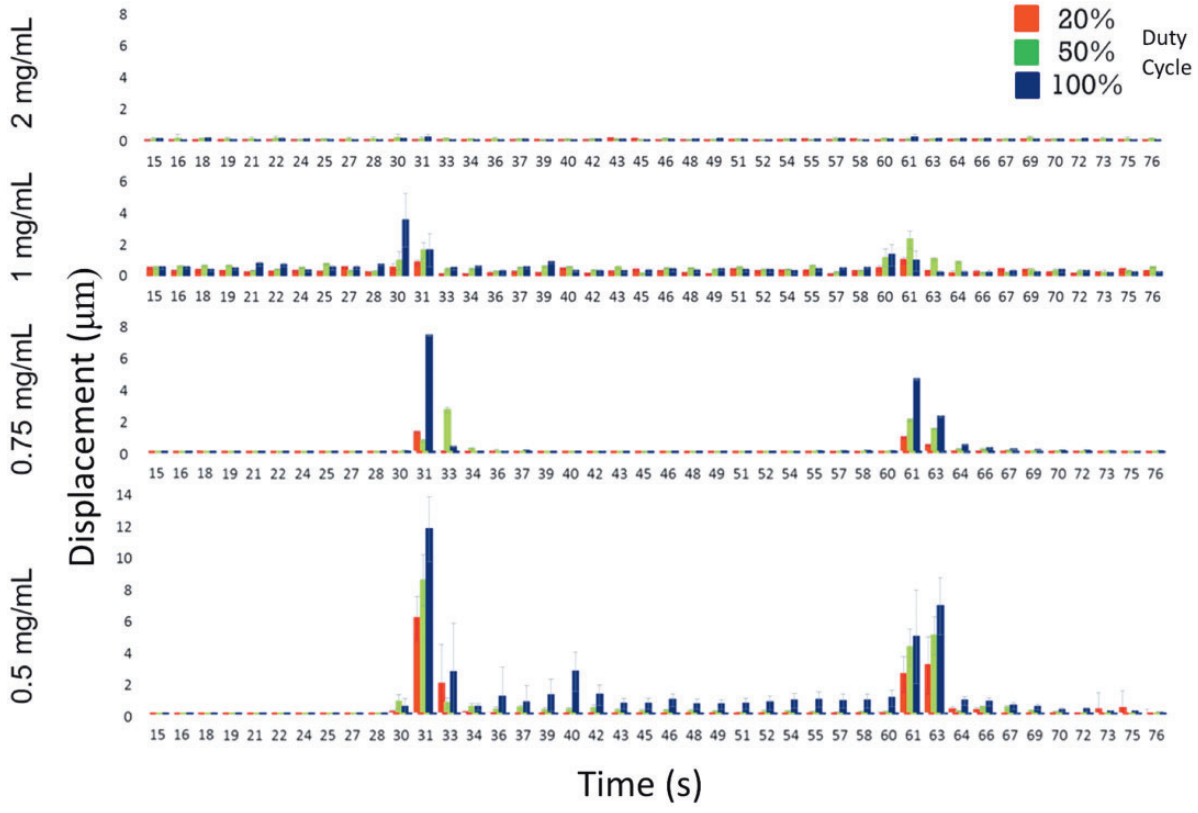

Figure 2 The displacement of individual beads encapsulated within the hydrogels was tracked and recorded using Volocity™ Software. The mean total displacement in the x, y, and z planes was recorded every second for 90 s; 30 s prior to the onset of ultrasound, 30 s during ultrasound, and 30 s after ultrasound had been turned off. For each hydrogel formulation and duty cycle, the displacement of 10 beads was tracked and recorded. Data show a relationship between hydrogel concentration and overall bead displacement, with lower concentrations of hydrogel showing larger bead displacements, and a relationship between increasing duty cycle and bead displacement, with higher duty cycles showing larger displacements within each hydrogel concentration. Evidence of bead displacement at 30 s, corresponding to the onset of ultrasound, and at 60 s, corresponding to the cessation of ultrasound, suggest that the hydrogels moved with the onset of ultrasound and then partially recovered their original shape after ultrasound. (A color version of this figure is available in the online journal.)

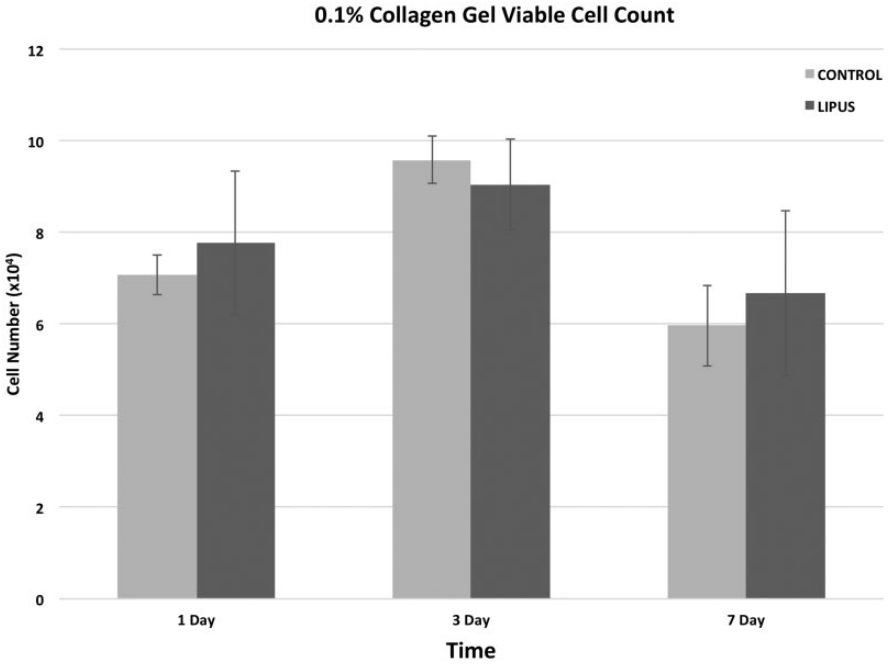

Figure 3 Proliferation studies of MC3T3 cells within 0.1% hydrogels shows no inhibitory (or proliferative) effect of ultrasound on the cells. No statistical difference was noted between proliferation of cells experiencing ultrasound and those not experiencing ultrasound at any time point ($p < 0.05$)

skin and soft tissue.[25] This has allowed it to be used as a minimally invasive therapeutic device for varied clinical indications depending on the overall intensity of the ultrasonic energy. One example is high-intensity focused ultrasound, which focuses acoustic energy at very high, sustained intensities (1–20 MW/cm^2) to destroy tissue by raising local tissue temperatures up to 100°C.[26] While sustained high intensities have limited applications as therapeutic tools, pulsed high intensities have been used to evaluate the mechanical properties of soft tissue through acoustic radiation force imaging,[27–30] a technique called elastography.[9] A very brief, very high-intensity acoustic wave (generally around 1–1000 W/cm^2)[31,32] is generated and propagated into a tissue that can physically displace that tissue anywhere from 8 to 400 μm,[27,28] which is in turn used to characterize the tissue's mechanical properties.[30] While intensities this high would be destructive to healthy tissue over extended periods of time, ultrasound at far lower intensities (<1 W/cm^2) has been shown to have a significant positive effect on fracture healing rates when applied to fresh fractures transdermally. This effect has lead to LIPUS being approved by the Food and Drug Administration for the treatment of fresh fractures (38% reduction in clinical and radiographic healing time) and fracture non-unions, and is being investigated for distraction osteogenesis.[33] Considerable work has been done to understand the mechanism behind this clinical efficacy by studying stem cells, osteoblasts, and osteocytes both *in vitro* and *in vivo* and much has been learned. *In vitro* studies have shown that LIPUS increases osteoblast cytokine production like vascular endothelial growth factor and fibroblast growth factor;[34] promotes chondrocyte aggrecan and type II procollagen synthesis;[35] inhibits osteoclastogenesis;[36] stimulates prostaglandin E_2 and COX-2 expression;[37] and elevates intracellular calcium, OC, DNA synthesis, and transforming growth factor-β synthesis as well.[38,39] What is still unknown is why these responses occur and whether

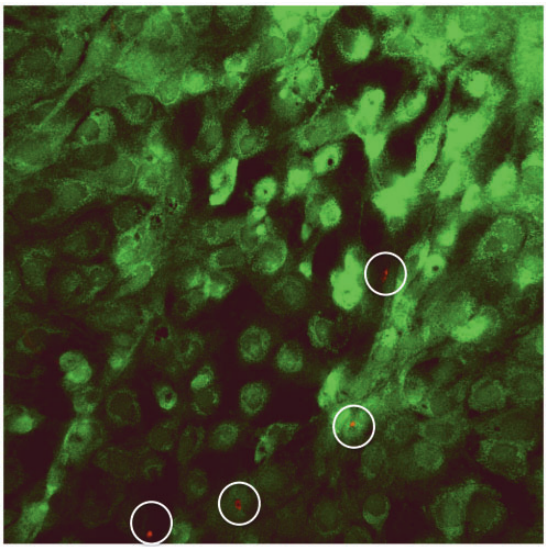

Figure 4 Live/dead assay indicating abundant cell viability 24 h after cell seeding. Viable cells appear green while dead cells appear red (mag = 10X)

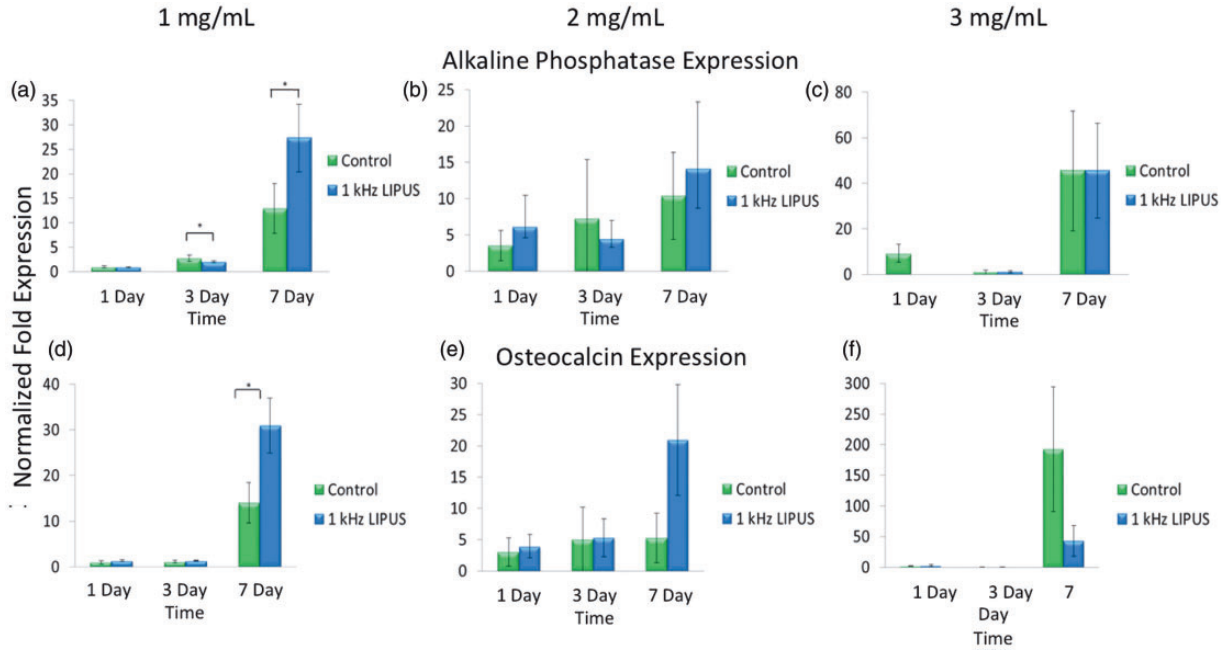

Figure 5 Gene expression of alkaline phosphatase and osteocalcin, both markers of osteoblastic differentiation, is shown to be elevated in cells encapsulated in 1 mg/mL collagen hydrogels after seven days of ultrasound exposure using the clinically prescribed spatial intensity (30 mW/cm^2) ($p < 0.05$) when compared to similarly encapsulated cells with no ultrasound exposure (a, d). As the concentration of hydrogel increases, and therefore the amount of hydrogel displacement noted in Figure 2 decreases, the gene expression of cells under ultrasound exposure is reduced to either match that of cells with no ultrasound (c) or to drop below (f) that of cells with no ultrasound, suggesting that as the displacement of hydrogels is reduced, so is the gene expression of both alkaline phosphatase and osteocalcin. (A color version of this figure is available in the online journal.)

being able to control cellular responses would further enhance healing.

In this study, we sought to determine if ultrasound, at its lowest clinically relevant intensities, does indeed manifest itself as a measurable physical load and if so, is capable of applying a strong enough physical load to deform collagen hydrogels capable of acting as cell delivery vehicles to facilitate bone repair. Further, we sought to examine whether cells encapsulated within collagen hydrogels would respond to ultrasound in a way that favored more rapid bone formation. Our results indicated that a measurable physical load does indeed arise from low-intensity ultrasound. We reported this load in Figure 1 as both a spatial intensity, which is the unit of measure used in therapeutic ultrasound for bone repair, and as a pressure. In either case the collected data would allow us to ''dial in'' the appropriate parameters such that the resulting ultrasonic energy will be as required.

Figure 2 demonstrates how the generated ultrasound was capable of displacing small fluorescent beads that were encapsulated within the hydrogels. The bead displacement magnitude was positively correlated with duty cycle such that as the duty cycle of the ultrasonic impulse increased from 20 to 50 to 100% so did the bead displacement. Displacement was inversely correlated with hydrogel concentration such that as the concentration (and similarly the mechanical stiffness) of the hydrogel increased bead displacement decreased. While these results appear intuitive they substantiate important claims that ultrasonic energy can be modulated to change the amount of deformation experienced by a hydrogel, allowing control over hydrogel deformation and, presumably, loading of encapsulated cells. We make the assumption that bead displacement equates to hydrogel deformation but are confident in this presumption because Figure 2 demonstrates that at the onset of ultrasound there is a measurable bead displacement, which we interpret as initial hydrogel deformation. During the ultrasound, however, there is little to no bead displacement, which we interpret as the hydrogel remaining deformed statically. At the cessation of ultrasound after 60 s there is another measurable bead displacement, which we interpret as the partial recovery of the hydrogel to its original shape. If there was no evidence of bead displacement at the cessation of ultrasound it would be difficult to argue that the beads mirrored hydrogel deformation, but given that the beads are displaced at the cessation of ultrasound, but also not to as great an extent as at its onset, we are confident that the hydrogel is moving with the beads and recovers partially, much like a viscoelastic material, which matches the mechanical behavior of the hydrogels after rheological evaluation (data not shown). If the beads were moving independently of the hydrogel we would expect the final displacement to equal the initial displacement or, since the beads are neutrally buoyant, show no final displacement at all.

Figure 3 demonstrates that ultrasound, in our experiments, had no effect on cell proliferation. This both corroborates[40] and contradicts[41] the literature as many variants of ultrasound have been tested. Further study confirmed that the cells did indeed survive within the hydrogels, as evidenced by Figure 4 in which live cells appear green and dead appear red. The vast majority of cells remain viable after being encapsulated within the hydrogel. Evaluating mRNA expression in response to applied ultrasound revealed an interesting point. While both AP and OC were upregulated after 14 days of daily ultrasound this response was mitigated, and even reversed, as the concentration of the hydrogel was increased. Increasing the collagen concentration in hydrogels corresponds to increased stiffness (data not shown) and also to decreased bead displacement (Figure 2). We surmised that over the relative long term (seven days) the physical response of osteoblasts to ultrasound can be muted by increasing the mechanical stiffness, and subsequently reducing the overall deformation, of the hydrogel within which the cells are encapsulated. This, along with the data presented in Figures 1 and 2 suggests three things: (1) ultrasound produces a measurable physical force that can be used to physically deform collagen hydrogels, (2) viable cells that are encapsulated within these hydrogels respond to the ultrasound-derived force by upregulating gene expression for key markers of bone cell differentiation typically seen as osteoblasts mature to bone forming cells, and (3) modifying the mechanical stiffness of these hydrogels can modulate the cellular response to the applied ultrasound. This work provides an important tool in cell therapy for bone repair by potentially allowing for the implantation of cells within a bony defect and the subsequent physical loading of those cells *after* implantation with control over the physical loading through either ultrasound modulation or hydrogel synthesis. This would allow for the physical stimulation of implanted cells during the earliest stages of fracture repair without disrupting the defect site when otherwise the complete immobilization would be mandated.

Authors' contribution: All authors participated in the design, interpretation of the studies, and analysis of the data. JV, FA, VV, BH, and YK conducted the experiments; LSN supplied intellectual guidance and expertise. JV, FA, and YK wrote the manuscript. LSN and BH reviewed and edited the manuscript.

ACKNOWLEDGEMENTS

The author(s) disclosed receipt of the following financial support for the research, authorship, and/or publication of this article: Research reported in this publication was supported by the National Institute of Arthritis and Musculoskeletal and Skin Diseases of the National Institutes of Health under Award Number AR064432-01A1. The content is solely the responsibility of the authors and does not necessarily represent the official views of the National Institutes of Health. The authors would like to thank Professor Hicham Drissi and Professor Peder Pedersen for their invaluable input and guidance at the outset of this project.

DECLARATION OF CONFLICTING INTERESTS

The author(s) declared no potential conflicts of interest with respect to the research, authorship, and/or publication of this article.

REFERENCES

1. Tibbitt MW, Anseth KS. Hydrogels as extracellular matrix mimics for 3D cell culture. *Biotechnol Bioeng* 2009;**103**:655–63
2. Wang C, Varshney RR, Wang D. Therapeutic cell delivery and fate control in hydrogels and hydrogel hybrids. *Adv Drug Deliv Rev* 2010;**62**:699–710
3. Nguyen KT, West JL. Photopolymerizable hydrogels for tissue engineering applications. *Biomaterials* 2002;**23**:4307–14
4. Lutolf MP, Hubbell JA. Synthetic biomaterials as instructive extracellular microenvironments for morphogenesis in tissue engineering. *Nat Biotechnol* 2005;**23**:47–55
5. Laurencin C, Khan Y, El-Amin SF. Bone graft substitutes. *Expert Rev Med Devices* 2006;**3**:49–57
6. Mazzocca AD, McCarthy MB, Chowaniec D, Cote MP, Judson CH, Apostolakos J, Solovyova O, Beitzel K, Arciero RA. Bone marrow-derived mesenchymal stem cells obtained during arthroscopic rotator cuff repair surgery show potential for tendon cell differentiation after treatment with insulin. *Arthroscopy* 2011;**27**:1459–71
7. Hoffman MD, Van Hove AH, Benoit DS. Degradable hydrogels for spatiotemporal control of mesenchymal stem cells localized at decellularized bone allografts. *Acta Biomater* 2014;**10**:3431–41
8. Gibbs DM, Black CR, Dawson JI, Oreffo RO. A review of hydrogel use in fracture healing and bone regeneration. *J Tissue Eng Regen Med* 2014;**10**:187-198
9. Brandenburg JE, Eby SF, Song P, Zhao H, Brault JS, Chen S, An KN. Ultrasound elastography: the new frontier in direct measurement of muscle stiffness. *Arch Phys Med Rehabil* 2014;**95**:2207–19
10. Malizos KN, Hantes ME, Protopappas V, Papachristos A. Low-intensity pulsed ultrasound for bone healing: an overview. *Injury* 2006;**37S**:S56–62
11. Giannoudis PV, Dinopoulos H, Tsiridis E. Bone substitutes: an update. *Injury* 2005;**36**:S20–7
12. Fleming JE, Cornell CN, Muschler GF. Bone cells and matrices in orthopedic tissue engineering. *Orthop Clin North Am* 2000;**31**:357–74
13. CDC first document Center for Disease Control: septic arthritis following anterior cruciate ligament reconstruction using tendon allografts—Florida and Louisiana, 2000. *Morb Mortal Wkly Rep* 2001;**50**:1081–3
14. CDC second document Center for Disease Control: Update: allograft-associated bacterial infections—United States, 2002. *Morb Mortal Wkly Rep* 2002;**51**:207–10
15. Wheeler DL, Enneking WF. Allograft bone decreases in strength in vivo over time. *Clin Orthop Rel Res* 2005;**435**:36–42
16. Ito H, Koefoed M, Tiyapatanaputi P, Gromov K, Goater JJ, Carmouche J, Zhang X, Rubery PT, Rabinowitz J, Samulski RJ, Nakamura T, Soballe K, O'Keefe RJ, Boyce BF, Schwarz EM. Remodeling of cortical bone allografts mediated by adherent rAAV-RANKL and VEGF gene therapy. *Nat Med* 2005;**11**:291–7
17. Dallari D, Fini M, Stagni C, Torricelli P, Nicoli Aldini N, Giavaresi G, Cenni E, Baldini N, Cenacchi, Bassi A, Giardino R, Fornasari PM, Giunti A. In vivo study on the healing of bone defects treated with bone marrow stromal cells, platelet-rich plasma, and freeze-dried bone allografts, alone and in combination. *J Orthop Res* 2006;**24**:877–88
18. Koefoed M, Ito H, Gromov K, Reynolds DG, Awad HA, Rubery PT, Ulrich-Vinther M, Soballe K, Guldberg RE, Lin AS, O'Keefe RJ, Zhang X, Schwarz EM. Biological effects of rAAV-caAlk2 coating on structural allograft healing. *Mol Ther* 2005;**12**:212–8
19. Fini M, Giavaresi G, Aldini NN, Torricelli P, Botter R, Beruto D, Giardino R. A bone substitute composed of polymethylmethacrylate and -tricalcium phosphate: results in terms of osteoblast function and bone tissue formation. *Biomaterials* 2002;**23**:4523–31
20. Kikuchi M, Itoh S, Ichinose S, Shinomiya K, Tanaka J. Self-organization mechanism in a bone-like hydroxyapatite/collagen nanocomposite synthesized in vitro and its biological reaction in vivo. *Biomaterials* 2001;**22**:1705–11
21. Chen F, Wang ZC, Lin CJ. Preparation and characterization of nano-sized hydroxyapatite particles and hydroxyapatite/chitosan nano-composite for use in biomedical materials. *Mater Lett* 2002;**57**:858–61
22. Borden M, Attawia M, Khan Y, Laurencin CT. Tissue engineered microsphere-based matrices for bone repair: design and evaluation. *Biomaterials* 2002;**23**:551–9
23. Khan Y, Katti DS, Laurencin CT. A novel polymer-synthesized ceramic composite based system for bone repair: osteoblast growth on scaffolds with varied calcium phosphate content. In: Laurencin CT, Botchwey E (eds) *Nanoscale materials science in biology and medicine*. MRS Proceedings Volume 845. Warrendale PA, Materials Research Society, 2005, pp. 63–67
24. Khan Y, Katti DS, Laurencin CT. A novel polymer-synthesized ceramic composite based system for bone repair: an in vitro evaluation. *J Biomed Mater Res* 2004;**69A**:728–37
25. Speed CA. Therapeutic ultrasound in soft tissue lesions. *Rheumatology* 2001;**40**:1331–36
26. Kennedy JE, Ter Haar GR, Cranston D. High intensity focused ultrasound: surgery of the future? *Br J Radiol* 2003;**76**:590–9
27. Nightingale KR, Palmeri ML, Nightingale RW, Trahey GE. On the feasibility of remote palpation using acoustic radiation force. *J Acoust Soc Am* 2001;**110**:625–34
28. Walker WF. Internal deformation of a uniform elastic solid by acoustic radiation force. *J Acoust Soc Am* 1999;**105**:2508–18
29. Erpelding TN, Hollman KW, O'Donnell M. Bubble-based acoustic radiation force elasticity imaging. *IEEE Trans Ultrason Ferroelectr Freq Control* 2005;**52**:971–9
30. Viola F, Walker WF. A spline-based algorithm for continuous time-delay estimation using sampled data. *IEEE Trans Ultrason Ferroelectr Freq Control* 2005;**52**:80–93
31. Nightingale K, Soo MS, Nightingale R, Trahey G. Acoustic radiation force impulse imaging: in vivo demonstration of clinical feasibility. *Ultrasound Med Biol* 2002;**28**:227–35
32. Walker WF, Fernandez FJ, Negron LA. A method of imaging viscoelastic parameters with acoustic radiation force. *Phys Med Biol* 2000;**45**:1437–47
33. Malizos KN, Hantes ME, Protopappas V, Papachristos A. Low-intensity pulsed ultrasound for bone healing: an overview. *Injury* 2006;**37S**:S56–62
34. Reher P, Elbeshir E-NI, Harvey W, Meghji S, Harris M. The stimulation of bone formation in vitro by therapeutic ultrasound. *Ultrasound Med Biol* 1997;**23**:1251–58
35. Parvizi J, Parpura V, Greenleaf JF, Bolander ME. Calcium signaling is required for ultrasound-stimulated aggrecan synthesis by rat chondrocytes. *J Orthop Res* 2002;**20**:51–57
36. Yang R-S, Lin W-L, Chen Y-Z, Tang C-H, Huang T-H, Lu B-Y, Fu W-M. Regulation by ultrasound treatment on the integrin expression and differentiation of osteoblasts. *Bone* 2005;**36**:276–83
37. Tang C, Yang R, Fu W. Prostaglandin E2 stimulates fibronectin expression through EP1 receptor, phospholipase C, protein kinase Cα, and c-Src pathway in primary rat osteoblasts. *J Biol Chem* 2005;**280**:22907–16
38. Day SM, Ostrum RF, Chao EYS, Rubin CT, Aro HT, Einhorn TA. Bone injury, regeneration, and repair. In Buckwalter JA, Eihnhorn TA, Simon SR (eds) *Orthopaedic basic science: biology and biomechanics of the musculoskeletal system*. American Academy of Orthopaedic Surgeons: Rosemont, IL, 2000, pp. 371–400
39. Caputo E. Healing of bone and connective tissues. In: Bronner F, Worrell RV (eds) *Orthopaedics: principles of basic and clinical science.* Boca Raton: CRC Press, 1999, pp. 201–216
40. Takayama T, Suzuki N, Ikeda K, Shimada T, Suzuki A, Maeno M, Otsuka K, Ito K. Low-intensity pulsed ultrasound stimulates osteogenic differentiation in ROS 17/2.8 cells. *Life Sci* 2007;**80**:965–71
41. Katiyar A, Randall L, Duncan RL, Sarkar K. Ultrasound stimulation increases proliferation of MC3T3-E1 preosteoblast-like cells. *J Ther Ultrasound* 2014;**2**:1